Available online at www.sciencedirect.com
SCIENCE DIRECT
Journal of Nuclear Materials 351 (2006) 56–64
journal of nuclear materials
www.elsevier.com/locate/jnucmat

Molecular dynamics simulation of primary irradiation defect formation in Fe–10%Cr alloy

Jae-Hyeok Shim [a,b,*], Hyon-Jee Lee [a], Brian D. Wirth [a]

[a] Department of Nuclear Engineering, University of California, Berkeley, CA 94720, USA
[b] Nano-Materials Research Center, Korea Institute of Science and Technology, Seoul 136-791, Republic of Korea

Abstract

Molecular dynamics simulations of displacement cascades in Fe and Fe–10%Cr have been performed for primary knock-on energies from 1 to 20 keV using two different Finnis–Sinclair style interatomic potentials. The different potentials were fit to describe the extremes of positive (attractive) and negative (repulsive) binding between substitutional Cr atoms and Fe self-interstitial atoms. As expected, the effect of Cr on the collisional stage of cascade evolution and on the number of point defects and point defect clusters produced is quite minimal. However, the quantity of mixed Fe–Cr dumbbells produced is sensitive to the choice of potential.

1. Introduction

High Cr ferritic/martensitic steels are candidates for first-wall and breeding-blanket structural materials in future fusion reactor systems. Therefore, fundamental understanding of microstructural evolution under conditions of fusion neutron irradiation is important, since microstructural changes will control mechanical behavior and performance. The modeling of primary defect formation by displacement cascades is a natural starting point in predicting neutron irradiation damage. Molecular dynamics (MD) simulations based on reliable semi-empirical many-body interatomic potentials have long been recognized as the most appropriate tool for the study of displacement cascades. To date many investigations have performed MD cascade simulations in pure Fe using a variety of interatomic potentials [1–4]. Cascade simulations in Fe alloys have been not been extensively studied, because reliable interatomic potentials for Fe alloys are limited.

However, specifically considering the Fe–Cr system, a couple of displacement cascade simulation studies have been performed very recently [5,6]. Malerba et al. [5] performed MD cascade simulations of pure Fe and Fe–10%Cr with primary knock-on atom (PKA) kinetic energies, E_p, of up to 15 keV using embedded atom method (EAM) potentials [7]. Malerba and co-authors used the Cr potential from the work of Farkas et al. [8], while

* Corresponding author. Address: Nano-Materials Research Center, Korea Institute of Science and Technology, Seoul 136-791, Republic of Korea. Tel.: +82 2 958 6760; fax: +82 2 958 5379.
E-mail address: jhshim@kist.re.kr (J.-H. Shim).

0022-3115/$ - see front matter © 2006 Elsevier B.V. All rights reserved.
doi:10.1016/j.jnucmat.2006.02.021

the Fe and Fe–Cr cross potentials were fit to available physical properties. Their results show that Cr atoms do not have a significant influence on the collision stage of cascades and the number of surviving defects. But, they did observe that mixed Fe–Cr dumbbells form preferentially in the Fe–10%Cr alloys. However, the Fe potential used in that work predicts incorrect stability of the self-interstitial atom in Fe, with the ⟨1 1 1⟩ dumbbell more stable than the ⟨1 1 0⟩ dumbbell [9], in disagreement with experimental observations [10], recent ab initio calculations [11,12] and most semi-empirical potentials [13–15].

Meanwhile, Wallenius et al. [6] recently fit embedded atom method (EAM)-style Fe–Cr potentials to various physical properties of pure Fe, pure Cr and Fe–Cr alloys. Wallenius and co-workers simulated displacement cascades of pure Fe, Fe–5%Cr and Fe–20%Cr with E_p up to 20 keV. Though the potentials of Wallenius et al. [6] are evidently improved and correctly predict the ⟨1 1 0⟩ dumbbell as the stable configuration in Fe, the calculated formation energy of the ⟨1 1 0⟩- and ⟨1 1 1⟩-oriented self-interstitial atoms (dumbbells) is more than twice as large as the recent ab initio calculations [11,12] and the experimental data [16]. Evidently, the large formation energy of self-interstitials was responsible for the much smaller number of surviving defects in their displacement cascade simulations [6], compared to other simulation results [1–5].

The purpose of this study is to construct an alternate set of Fe–Cr potentials, that predict the correct relative stability of self-interstitials with more appropriate formation energies; and to elucidate the effect of Cr atoms on primary irradiation defect formation in an Fe–10%Cr alloy by performing MD simulations of displacement cascades. Section 2 describes the fitting procedure used to develop the interatomic potentials. Section 3 presents a discussion of the cascade simulation results in pure Fe and an Fe–10%Cr alloy for PKA energies from 1 to 20 keV, and for two different parameterizations of the Fe–Cr potential which give opposite interactions between Cr and self-interstitial atoms. The results are summarized in Section 4.

2. Interatomic potentials and simulation methods

The Finnis–Sinclair potential formalism [17], which provides a similar framework to the EAM, was chosen to construct the Fe–Cr potentials. In the framework of the Finnis–Sinclair approach, the total energy of the system of n atom is given by

$$E_{\text{tot}} = \frac{1}{2}\sum_{i\neq j}^{n} V_{ij}(R_{ij}) - \sum_{i}^{n}\left\{\sum_{j}^{n}\phi_{ij}(R_{ij})\right\}^{1/2}, \qquad (1)$$

where V_{ij} and ϕ_{ij} are the pairwise repulsive and the many-body cohesive interactions, respectively, between atoms i and j separated by a distance R_{ij}.

The potentials for the pure elements were taken from the literature [14,17], using the potentials fit by Ackland et al. [14] for Fe and by Finnis and Sinclair [17] for Cr. For cascade simulations, it is important to validate a potential at short atomic separations as well as near the equilibrium lattice spacings. For instance, it is known that the Fe potential developed by Finnis and Sinclair [17] is too 'soft' at short atomic separations and therefore not well suited for MD simulations of high-energy cascades. Calder and Bacon [1] modified this potential to make it 'stiffer' in their cascade simulations. Fortunately, the Finnis–Sinclair type Fe potential proposed later by Ackland et al. [14] already includes such a modification at short atomic separations and is appropriate for cascade simulations. The Ackland Fe potential [14] also correctly predicts the stability and defect formation energy of self-interstitial atoms, although more recent ab initio calculations [12] and Finnis–Sinclair type Fe potential by Mendelev et al. [15] predict a larger energy difference between SIAs in the form of ⟨1 1 0⟩ and ⟨1 1 1⟩-oriented split dumbbells and a change in the SIA migration mechanism. Fig. 1 plots the volume–energy curve of the Finnis–Sinclair Cr potential [17] and shows reasonably good agreement with the universal equation of state [18].

To construct the Fe–Cr cross potential, the two terms V_{FeCr} and ϕ_{FeCr} need to be determined. The method proposed by Konishi et al. [19] was adopted from the various cross potential schemes. According to this approach, the two terms are given by

$$\phi_{\text{FeCr}} = \alpha\sqrt{\phi_{\text{FeFe}}\phi_{\text{CrCr}}}, \qquad (2)$$

$$V_{\text{FeCr}} = \frac{\beta}{2}\left(\frac{\phi_{\text{FeCr}}}{\phi_{\text{FeFe}}}V_{\text{FeFe}} + \frac{\phi_{\text{FeCr}}}{\phi_{\text{CrCr}}}V_{\text{CrCr}}\right), \qquad (3)$$

where α and β are adjustable fitting parameters.

In this study, α and β were fit to experimental data including the enthalpy of mixing and the variation of lattice constants in Fe–Cr alloys as a function of Cr content. The fitted parameters are given in Table 1. The first attempt involved fitting only

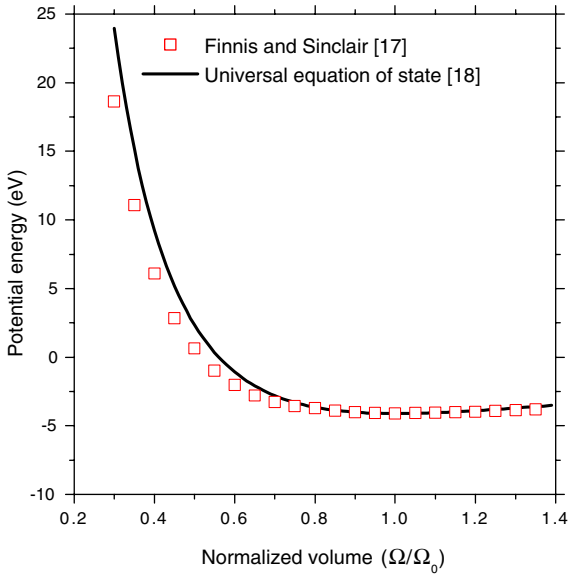

Fig. 1. Calculated potential energy of Cr versus atomic volume, as calculated using the Finnis–Sinclair Cr potential [17] and compared to the universal equation of state [18].

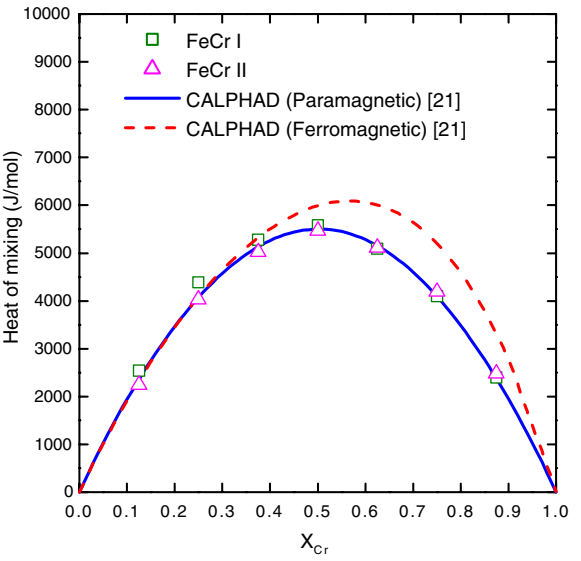

Fig. 2. Heat of mixing in Fe–Cr bcc alloys calculated by the present Fe–Cr potentials, and compared to the calculations from CALPHAD for both ferromagnetic and paramagnetic Fe–Cr alloys.

Table 1
Parameters for the Fe–Cr potential fitted in this study

	α	β
FeCr I	1.00	1.25
FeCr II	0.94	0.90

β, with α fixed equal to 1, which is equivalent to the original approach proposed by Ackland and Vitek [20] for fitting alloy potentials within the Finnis–Sinclair framework. This potential will be referred to throughout the paper as FeCr I. Fig. 2 shows the heat of mixing predicted by the FeCr I potential, in addition to the values calculated by the CALPHAD approach [21] for both paramagnetic and ferromagnetic alloys, which are derived from experimental data [22]. The FeCr I potential is in very good agreement with the calculated mixing enthalpies for paramagnetic alloys for all Cr concentrations and is also in excellent agreement with the calculated mixing enthalpy of ferromagnetic alloys in the Fe-rich region ($X_{Cr} < \sim 0.4$). Fig. 3 shows a comparison of the lattice parameter calculated from the FeCr I potential for pure Fe and four different Fe–Cr alloys with three different sets of experimental data (shown as trend-lines) [23–25]. The experimental data shows considerable scatter with increasing Cr concentration, but the predictions of the FeCr I potential are in very good agreement

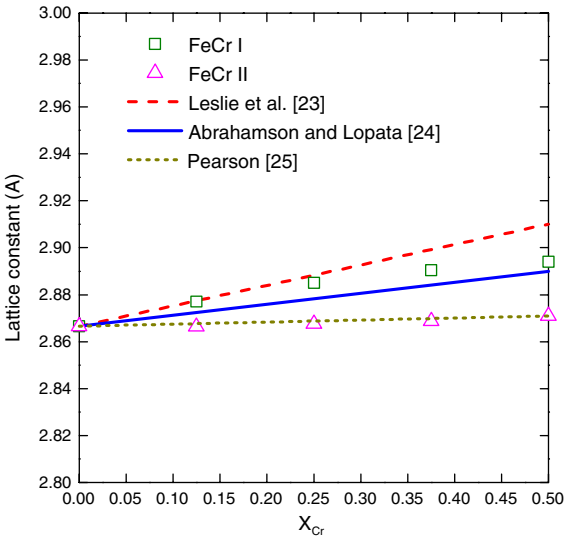

Fig. 3. Calculated lattice constants in Fe–Cr bcc alloys by the present Fe–Cr potentials in comparison with the experimental data.

with the data of Pearson [25]. The binding energies of Cr atoms with vacancy and interstitial point defects are presented in Table 2, in addition to the value of the $\langle 110 \rangle$-oriented Fe–Cr mixed dumbbell published by Wallenius et al. [6] and ab initio calculations by Domain [26]. The binding energies of Fe–Cr $\langle 110 \rangle$ and $\langle 111 \rangle$ mixed dumbbells with respect

Table 2
Calculated binding energies of Cr-vacancy, Cr–Cr and Cr-dumbbells in bcc Fe relative to well-separated Cr and point defects

	F–S FeCr I	F–S FeCr II	EAM, Wallenius [6]	Ab initio, Domain [26]
Cr–V 1NN	0.04	−0.002	–	–
Cr–V 2NN	−0.04	−0.01	–	–
Cr–Cr 1NN	0.07	0.03	–	–
Cr–Cr 2NN	0.0004	0.03	–	–
$\langle 1\,1\,0\rangle I_{FeCr}$	−0.40	0.10	0.27	0
$\langle 1\,1\,1\rangle I_{FeCr}$	−0.25	0.20	–	0.3
$\langle 1\,1\,0\rangle I_{FeFe}$–Cr (parallel)	−0.16	0.06	–	–
$\langle 1\,1\,0\rangle I_{FeFe}$–Cr (perpendicular)	0.02	−0.007	–	–

All energies are given in eV.

to a well-separated Cr atom and SIA are −0.40 and −0.25 eV, respectively and the negative values mean that these dumbbells are not energetically stable compared to the Fe SIA. However, this is opposite to a recent ab initio calculation which predicts a zero binding energy for the $\langle 1\,1\,0\rangle$ and a positive binding energy of 0.3 eV for the $\langle 1\,1\,1\rangle$-oriented mixed dumbbells [26]. As well, the Fe–Cr potential of Wallenius et al. [6] predicts a relatively large positive binding energy of 0.27 eV for the $\langle 1\,1\,0\rangle$-oriented mixed dumbbell.

Thus, it was decided to make another Fe–Cr potential that would predict a positive binding energy for the mixed interstitial dumbbell configurations by fitting both α and β simultaneously. This potential was named FeCr II. The FeCr II potential does predict positive binding energies for the mixed dumbbells, as described in Table 2, in addition to providing very good agreement with the enthalpy of mixing and reasonable agreement with the lattice parameter of Fe–Cr alloys as a function of Cr content, as shown in Figs. 2 and 3. As a first attempt to validate these two potentials and to determine which is most appropriate for simulating Cr-point defect interactions and defect production by displacement cascades in Fe–Cr alloys, an ab initio calculation was carried out using the SeqQuest code [27]. The SeqQuest performs the density functional theory (DFT) calculations using norm-conserving pseudopotentials and Gaussian basis sets in a linear combination of atomic orbitals (LCAO) approach. For the present calculations, the Perdew–Burke–Ernzerhof [28] generalized gradient approximation (PBE-GGA) with spin-polarized scheme is used. This ab initio calculation involved placing a single substitutional Cr atom in a bcc Fe matrix consisting of 54 atoms. Although Cr is expected to be a slightly oversized atom compared to Fe, the SeqQuest calculation predicts that the first nearest neighbor Fe atoms constrict toward the Cr atom by 0.3%. This is in better agreement with the prediction of the FeCr II potential, as shown in Table 3 and may be closely related with the recent ab initio calculation by Domain that predicts the formation of energetically stable mixed Fe–Cr dumbbells in Fe [26]. However, the energetic stability of the mixed dumbbells is not well understood at this time, especially considering that Cr is slightly oversized and elastically stiffer than Fe [17]. It is possible that this behavior is caused by complex electronic or magnetic interactions between Fe and Cr in Fe-rich regions, but complete understanding will require further electronic structure calculations. At this time, we note only that the FeCr II potential is in reasonably good agreement with available experimental information and the recent ab initio calculations, and we compare the point defect production behavior predicted by the two different potentials in an Fe–10%Cr alloy for displacement cascades initiated by primary knock-on atoms with kinetic energy from 1 to 20 keV.

The two Fe–Cr potentials that have been developed were implemented in the MDCASK code [29] and MD simulations were performed using a constant pressure periodic boundary condition based on the Parrinello–Rahman method [30]. The computational cell is composed of $60 \times 60 \times 60$ bcc

Table 3
Change in first nearest neighbor distance around a substitutional Cr atom in bcc Fe

	Change (%)
FeCr I	+0.53
FeCr II	−0.32
Ab initio (SeqQuest)	−0.29

unit cells (432 000 atoms). The cell was thermally equilibrated at 673 K for 30 ps prior to performing the cascade simulations. The cascades were initiated by giving a PKA kinetic energy, E_p, ranging from 1 to 20 keV along ⟨1 3 5⟩ directions in pure Fe and Fe–10%Cr alloys. The MD simulations continued for 40 ps without temperature rescaling after starting cascades. In order to obtain statistically meaningful results, 5–10 MD runs were carried out at each kinetic energy by changing the specific PKA direction. The Wigner–Seitz cell method was adopted to analyze the number and distribution of produced defects. Second nearest neighbor (NN) and third NN criterion were used to define vacancy and interstitial atom clusters, respectively.

3. Results and discussion

Fig. 4 plots the variation in the average number of Frenkel pairs with time during a 20 keV displacement cascade in pure Fe and in an Fe–10%Cr alloy, with the FeCr I and FeCr II potentials. Very similar behavior is observed, independent of the Cr content (similar for pure Fe and Fe–10%Cr) or the interatomic potential used to describe the Fe–Cr interaction (FeCr I and FeCr II). The number of Frenkel pairs initially increases rapidly until reaching a peak about 0.5 ps after initiation of the cascade. The number of Frenkel pairs at the peak of this collisional stage is between 800 and 900. Subsequently, the number of Frenkel pairs decreases rapidly due to interstitial-vacancy recombination and then slowly decreases for times greater than about 6 ps. These results indicate that Cr atoms in Fe do not have a significant effect on the number of primary irradiation defects forming during cascades, as expected from other works [5,6].

The average number of Frenkel pairs surviving after 40 ps is plotted in Fig. 5 as a function of E_p. The variation of defect production with PKA energy is well described by the power law fit proposed by Bacon et al. [31] for pure Fe, and indeed, a similar power law exponent of 0.8 ± 0.02 is observed, although a slightly smaller prefactor of 3.5 versus 5.7 is obtained in this study. The defect production efficiency is presented in Fig. 6 by dividing the number of surviving Frenkel pairs into the displacement predicted by the Norgett–Robinson–Torrens (NRT) model [32]. According to the NRT model, the number of Frenkel pairs produced by a PKA of kinetic energy E_p is defined as $0.8E_p/2E_d$, where E_d is the average threshold displacement energy an the recommended value of $E_d = 40$ eV for bcc Fe is used [2]. Although there are relatively large statistical uncertainties at low energies, the overall trend in the defect production efficiency is to slowly decrease as E_p increases, as is observed in other studies [5]. The efficiency at 20 keV is about 0.22, which is slightly lower than the previous works for pure Fe [2] and Fe–10%Cr [5].

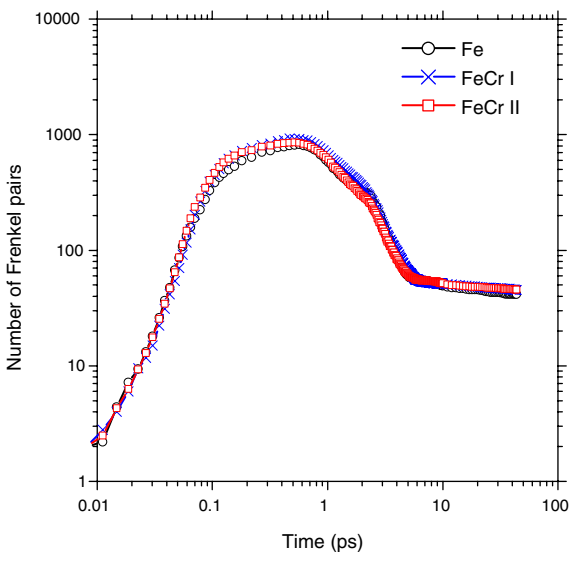

Fig. 4. Number of Frenkel pairs versus time during 20 keV cascade.

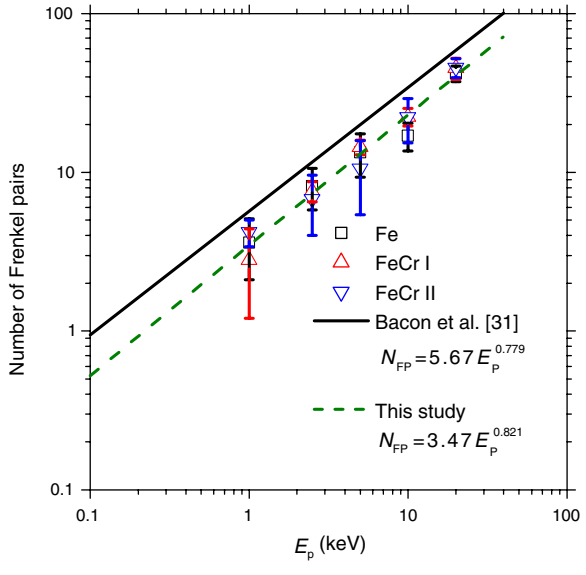

Fig. 5. Number of Frenkel pairs versus primary knock-on atom energy, E_p.

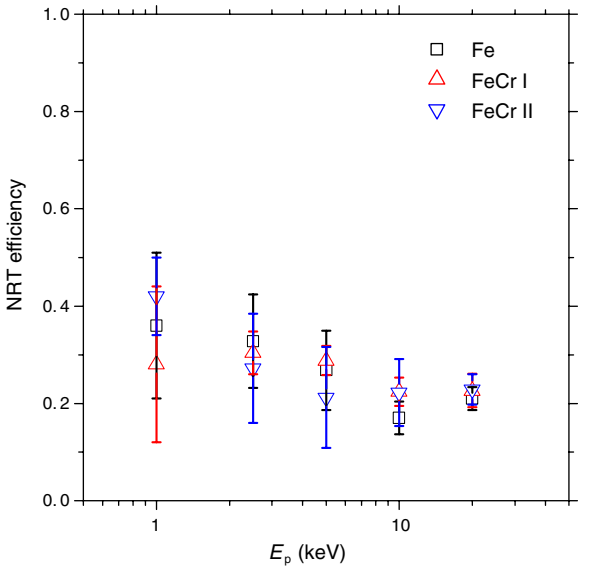

Fig. 6. Defect production efficiency versus primary knock-on atom energy, E_p.

Fig. 7 shows the typical defect distribution for pure Fe and Fe–10%Cr at a time of 40 ps after the 20 keV cascades. No significant difference in the defect distribution between pure Fe and the Fe–10%Cr alloy is found. While most vacancies are isolated, many of the interstitial atoms form clusters containing two or more interstitials. Very large clusters containing more than 10 interstitials are found in all cases. FeCr I and FeCr II exhibit an opposite feature with respect to the chemistry around the defects, as is expected from the Cr-interstitial binding energies (Table 2). Many Fe–Cr mixed and even Cr–Cr dumbbells are produced using the FeCr II potential, whereas mixed dumbbells are not observed in the FeCr I potential, as expected from the negative Cr–SIA binding energy, and most dumbbells are Fe–Fe. However, Cr atoms are often found in very large SIA clusters, even using the FeCr I potential, which is different than the behavior of single interstitials. Fig. 8 plots the average number of Fe–Fe, Fe–Cr and Cr–Cr interstitial dumbbells as a function of PKA energy. As expected, the fraction of mixed dumbbells, and even Cr–Cr dumbbells is much larger for the FeCr II than the FeCr I potentials. Further, the fraction of mixed dumbbells observed in cascades using the FeCr II potential are substantially greater than the number expected based on the probability of finding a Cr atom as part of an interstitial dumbbell in a randomly distributed 10% Cr alloy, which would be 0.2.

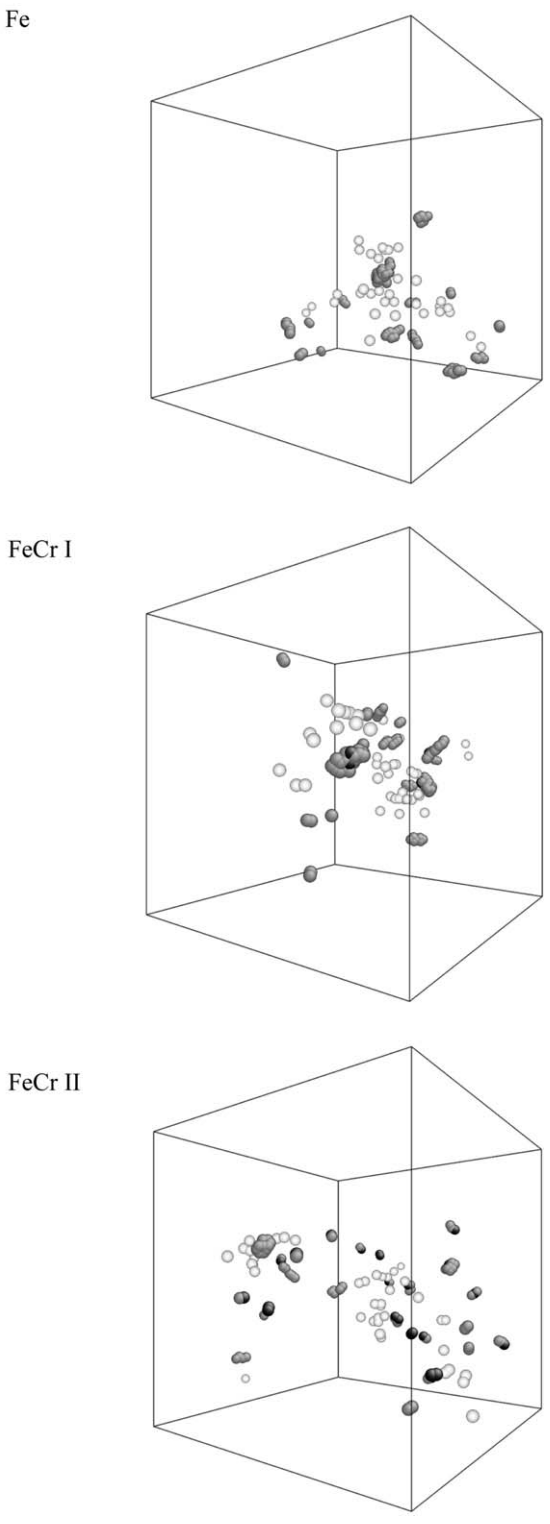

Fig. 7. Typical defect distributions at 40 ps after 20 keV cascades. The empty, gray and black circles represent vacancies, Fe SIAs and Cr SIAs, respectively.

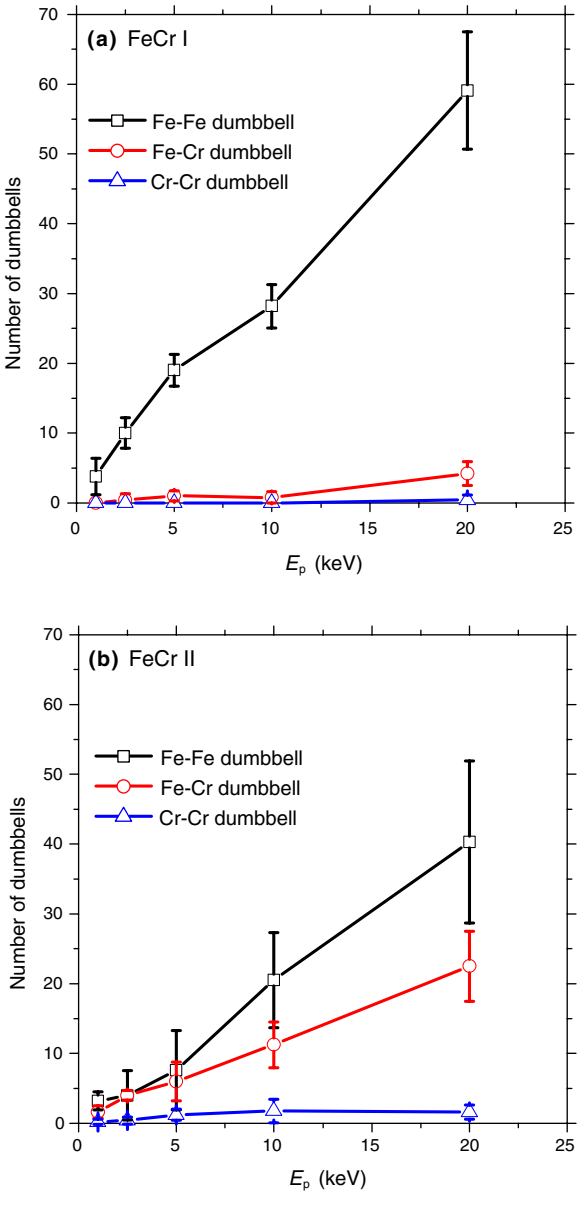

Fig. 8. The average number of Fe–Fe, Fe–Cr and Cr–Cr dumbbells in Fe–10%Cr alloys produced in a 20 keV cascade: (a) FeCr I and (b) FeCr II.

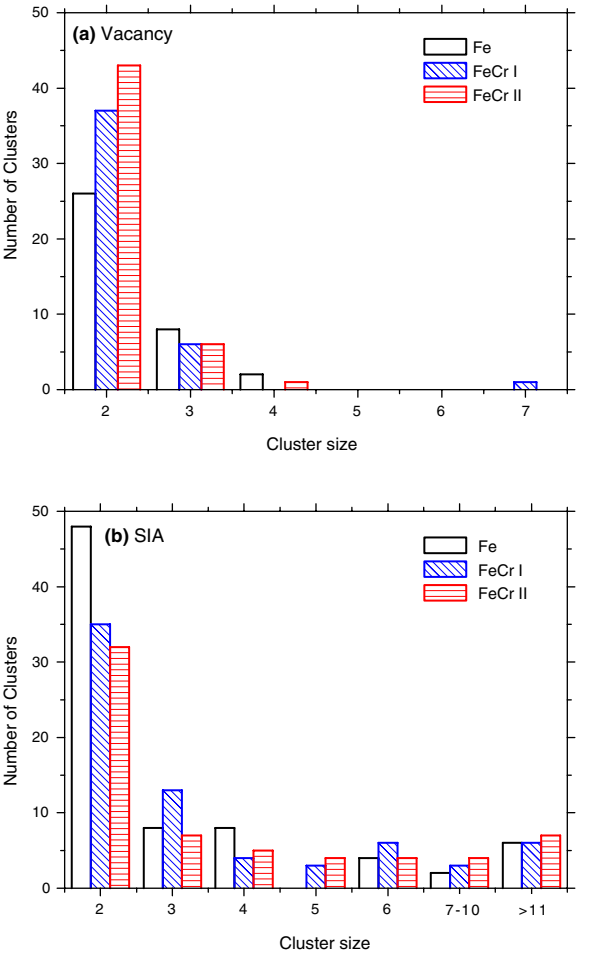

Fig. 9. The size distributions of (a) vacancy and (b) interstitial clusters produced in a 20 keV cascade.

The vacancy and SIA cluster size distributions at a PKA energy of 20 keV are presented in Fig. 9. Consistent with previous MD cascade simulations in pure Fe [4], most of the vacancies are isolated, but those in clusters primarily contain only 2 or 3 vacancies. As shown in Fig. 9(a), the number of di-vacancy clusters in the Fe–10%Cr alloy is larger than observed in pure Fe for both FeCr I and FeCr II. For interstitial clusters, a much wider cluster size distribution is obtained, although it is still peaked at a cluster size of 2. The agreement between pure Fe and the Fe–10%Cr alloy is much better for the interstitial size distribution than for the vacancy cluster size distribution, although the underlying reason for the difference is not clear. Fig. 10 shows the average fraction of vacancies and interstitials in clusters (shown in percent) as a function of E_p. A very large scatter exists in the obtained simulation results, especially for the lower PKA energies. While there is no clear trend in the fraction of vacancy clusters with PKA energy, the range of values of from 5% to 25% agree well with the values obtained by Becquart et al. [4] in Fe–Cu alloys. The fraction of interstitials in clusters increases with increasing E_p until reaching an apparent saturation of about 65% for PKA energies above about 5 keV. This tendency is in agreement with the behavior observed in pure Fe cascade simulations by Stoller et al. [2]

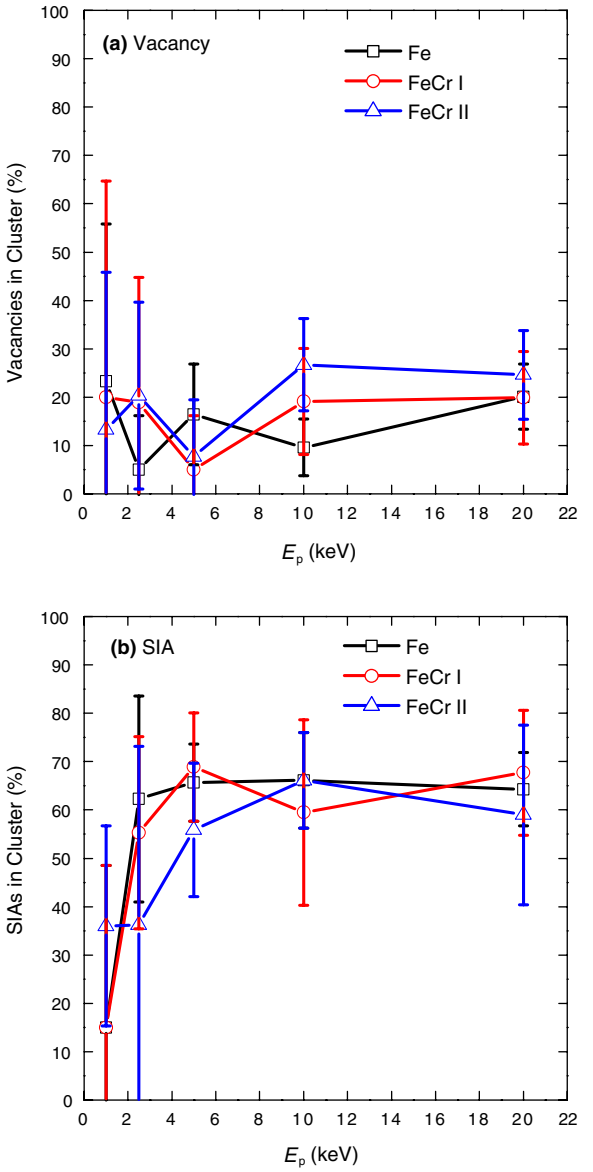

Fig. 10. Fraction of (a) vacancies and (b) interstitials in clusters versus primary knock-on atom energy, E_p.

using the original Finnis–Sinclair Fe potential. However, the fraction of interstitials in clusters obtained in this work is slightly larger compared to the more recent Fe–Cr cascades simulations of Malerba et al. [5].

The results of this study indicate that Cr atoms in an Fe–10%Cr alloy do not have a significant effect on either the number of defects formed or on the number of point defect clusters produced during displacement cascades with PKA energies from 1 to 20 keV. This is consistent with the results of other cascade simulation studies in pure Fe and Fe alloys [5,6]. However, the subsequent microstructural evolution during the long-time annealing or aging evolution of the cascades [33,34] is much more likely to be influenced by the Cr atoms, since Cr and other solutes can have a much stronger effect on defect mobility, particularly for interstitial atoms and interstitial clusters. Recent MD simulations in Fe–Cr [9] and Fe–Cu [35] alloys have shown changes in the (self-) interstitial atom diffusivity by the presence of solute atoms. In addition, recent experimental observations indicate that Cr can retard the one-dimensional motion of interstitial dislocation loops in Fe [36]. It is generally believed that the binding energy between self-interstitial and solute atoms will be the main factor controlling changes in the SIA diffusivity. The two interatomic Fe–Cr potentials proposed in this study show opposite binding interactions for Fe–Cr mixed dumbbells and can provide insight into the effects of solute atoms with different binding energies on interstitial and interstitial atom diffusivity. At the present time, it is difficult to determine whether the FeCr I or FeCr II potential is most appropriate for simulations of point defect and in particular, interstitial, mobility in Fe–Cr alloys, although the recent ab initio calculations support FeCr II. Additional ab initio calculations, as well as experimental investigations into the stability and mobility of interstitial atoms, and kinetic models that can predict microstructural evolution during irradiation and isochronal annealing with the two extremes of Cr-interstitial binding and compare to previous experimental studies of isochronal annealing recovery of electron irradiated Fe–Cr alloys are required to validate these potentials.

4. Conclusions

MD simulations of displacement cascades with primary knock-on atom kinetic energy from 1 to 20 keV have been performed in Fe and an Fe–10%Cr alloy with potentials based on the Finnis–Sinclair formalism. Two different cross potentials for Fe–Cr, FeCr I and FeCr II, have been fit to the available experimental information, including the heat of mixing and variations in the lattice constant with Cr additions to Fe–Cr alloys. The two potentials exhibit opposite behavior for the Cr-interstitial atom interaction; the FeCr I potential predicts a negative binding energy for Fe–Cr mixed dumbbells, while the FeCr II potential predicts the stable formation of mixed dumbbells. The potentials used in this study show slightly lower NRT

defect production efficiency compared to previous cascade studies on pure Fe and Fe–Cr alloys. As expected, Cr atoms do not have much influence on defect population during the cascade collisional stage, regardless of which Fe–Cr potential is selected. However, the effect of Cr-interstitial atom binding energy is readily apparent with the large number (35% at 20 keV) of mixed Fe–Cr dumbbells produced in displacement cascades simulated with the FeCr II potential. However, the mixed dumbbell fraction is lower than the results of Malerba et al. [5]. While Cr atoms did not have a strong influence on the displacement cascade evolution during the initial 40 ps, a larger influence of Cr is anticipated on the mobility of interstitial atoms and interstitial clusters and the subsequent aging evolution of the cascade defect structure, which will be investigated in the future using kinetic Monte Carlo simulations.

Acknowledgements

This work has been supported by the Office of Fusion Energy Sciences, US Department of Energy under Grant DE-FG02-04ER54750. The authors would like to thank Dr Peter A. Schultz for many helpful discussions related to the use of the SeqQuest code.

References

[1] A.F. Calder, D.J. Bacon, J. Nucl. Mater. 207 (1993) 25.
[2] R.E. Stoller, G.R. Odette, B.D. Wirth, J. Nucl. Mater. 251 (1997) 49.
[3] N. Soneda, T. Diaz de la Rubia, Philos. Mag. A 78 (1998) 995.
[4] C.S. Becquart, C. Domain, A. Legis, J.C. Van Duysen, J. Nucl. Mater. 280 (2000) 73.
[5] L. Malerba, D. Terentyev, P. Olsson, R. Chakarova, J. Wallenius, J. Nucl. Mater. 329–333 (2004) 1156.
[6] J. Wallenius, P. Olsson, C. Lagerstedt, N. Sandbers, R. Chakarova, V. Pontikis, Phys. Rev. B. 69 (2004) 094103.
[7] M.S. Daw, M.I. Baskes, Phys. Rev. Lett. 50 (1983) 1285.
[8] D. Farkas, C.G. Schon, M.S.F. de Lima, H. Goldstein, Acta Mater. 44 (1996) 409.
[9] D. Terentyev, L. Malerba, J. Nucl. Mater. 329–333 (2004) 1161.
[10] H. Maeta, F. Ono, T. Kittaka, J. Phys. Soc. Jpn. 53 (1984) 4353.
[11] C. Domain, C.S. Becquart, Phys. Rev. B. 65 (2001) 024103.
[12] C.-C. Fu, F. Willaime, P. Ordejón, Phys. Rev. Lett. 92 (2004) 175503.
[13] B.D. Wirth, G.R. Odette, D. Maroudas, G.E. Lucas, J. Nucl. Mater. 244 (1997) 185.
[14] G.J. Ackland, D.J. Bacon, A.F. Calder, T. Harry, Philos. Mag. A 75 (1997) 713.
[15] M.I. Mendelev, S. Han, D.J. Srolovitz, G.J. Ackland, D.Y. Sun, M. Asta, Philos. Mag. 83 (2003) 3977.
[16] H.J. Wollenberger, in: R.W. Cahn, P. Haasen (Eds.), Physical Metallurgy, 3rd Ed., Elsevier, Amsterdam, 1983, p. 1139.
[17] M.W. Finnis, J.E. Sinclair, Philos. Mag. A 50 (1984) 45.
[18] J.H. Rose, J.R. Smith, F. Guinea, J. Ferrante, Phys. Rev. B 29 (1984) 2963.
[19] T. Konishi, K. Ohsawa, H. Abe, E. Kuramoto, Comput. Mater. Sci. 14 (1999) 108.
[20] G.J. Ackland, V. Vitek, Phys. Rev. B 41 (1990) 10324.
[21] J.-O. Andersson, B. Sundman, Calphad 11 (1987) 83.
[22] W.A. Dench, Trans. Faraday Soc. 59 (1963) 1279.
[23] W. Leslie, R.J. Sober, S.G. Babcock, S.J. Green, Trans. Am. Soc. Met. 62 (1969) 690.
[24] E.P. Abrahamson, S.L. Lopata, Trans. Metall. Soc. AIME 236 (1966) 76.
[25] W.B. Pearson, A Handbook of Lattice Spacings and Structures of Metals and Alloys, Pergamon, New York, 1958, p. 532.
[26] C. Domain, private communication.
[27] http://www.cs.sandia.gov/~paschul/Quest.
[28] J.P. Perdew, K. Burke, M. Ernzerhof, Phys. Rev. Lett. 77 (1996) 3865.
[29] T. Diaz de la Rubia, M.W. Guinan, J. Nucl. Mater. 174 (1990) 151.
[30] M. Parrinello, A. Rahman, Phys. Rev. Lett. 45 (1980) 1196.
[31] D.J. Bacon, A.F. Calder, F. Gao, V.G. Kapinos, S.J. Wooding, Nucl. Instrum. and Meth. B 102 (1995) 37.
[32] M.J. Norgett, M.T. Robinson, I.M. Torrens, Nucl. Eng. Des. 33 (1975) 50.
[33] F. Maury, P. Lucasson, A. Lucasson, F. Faudot, J. Bigot, J. Phys. F: Met. Phys. 17 (1987) 1143.
[34] H. Abe, E. Kuramoto, J. Nucl. Mater. 271&272 (1999) 209.
[35] J. Marian, B.D. Wirth, J.M. Perlado, G.R. Odette, T. Diaz de la Rubia, Phys. Rev. B 64 (2001) 094303.
[36] K. Arakawa, M. Hatanaka, H. Mori, K. Ono, J. Nucl. Mater. 329–333 (2004) 1194.